perature of a *partially* equilibrated system may not tend to increase much.) As it is seen from Fig. 1(b), the calculated excitation functions reproduce well the energy thresholds and absolute cross sections for both (^{12}C, α) and (^{12}C, 2α) incomplete-fusion reactions.

The proposed model can be checked more extensively using our new data on the ^{14}N + ^{159}Tb system. The absolute cross sections for a number of capture reactions (see Table I) are compared with the model predictions if we assume the same set of parameters as that used for the ^{12}C + ^{160}Gd system. The calculated cross sections are given also for other channels for which we could not determine the cross sections. [For instance, we were not able to measure the compound-residue cross section since the (^{14}N, xn) channels in the ^{14}N + ^{159}Tb reaction at 140 MeV lead to unknown isotopes of Hf.] There is a close correlation between the calculated and measured cross sections. This result strongly indicates that both the Q_{gg} effects and the entrance-channel limitations built into the model influence the cross sections.

The analysis of the experimental data on the ^{12}C + ^{160}Gd and ^{14}N + ^{159}Tb systems gives strong arguments in support of the proposed model. An intriguing question is whether the mass and charge distributions of the products of strongly damped reactions in collisions of very heavy systems can also be described by this model. The proposed model couples strongly the complete-fusion reactions with other reaction modes. [Actually, the sum rule (7) simulates in a sense a complete coupled-channels calculation in the no-imaginary-potential limit.] Such an approach offers, therefore, a possible explanation of the nuclear structure effects which show up in magnitudes of the fusion cross sections especially for light systems.[13]

[a]Permanent address: Institute of Nuclear Research, 05-400 Świerk, Poland.

[1]K. Siwek-Wilczyńska, E. H. du Marchie van Voorthuysen, J. van Popta, R. H. Siemssen, and J. Wilczyński, Phys. Rev. Lett. 42, 1599 (1979).

[2]K. Siwek-Wilczyńska, E. H. du Marchie van Voorthuysen, J. van Popta, R. H. Siemssen, and J. Wilczyński, Nucl. Phys. A330, 150 (1979).

[3]K. A. Geoffroy, D. G. Sarantites, M. L. Halbert, D. C. Hensley, R. A. Dayras, and J. H. Barker, Phys. Rev. Lett. 43, 1303 (1979).

[4]T. Inamura, M. Ishihara, T. Fukuda, T. Shimoda, and H. Hiruta, Phys. Lett. 68B, 51 (1977).

[5]D. R. Zolnowski, H. Yamada, S. E. Cala, A. C. Kahler, and T. T. Sugihara, Phys. Rev. Lett. 41, 92 (1978).

[6]H. Yamada, D. R. Zolnowski, S. E. Cala, A. C. Kahler, J. Pierce, and T. T. Sugihara, Phys. Rev. Lett. 43, 605 (1979).

[7]A. G. Artukh, V. V. Avdeichikov, J. Erö, G. F. Gridnev, V. L. Mikheev, V. V. Volkov, and J. Wilczyński, Nucl. Phys. A160, 511 (1971).

[8]J. P. Bondorf, F. Dickmann, D. H. E. Gross, and P. J. Siemens, J. Phys. (Paris), Colloq. 32, C6-145 (1971).

[9]J. Wilczyński, Nucl. Phys. A216, 386 (1973).

[10]D. Glass and U. Mosel, Nucl. Phys. A237, 429 (1975).

[11]J. Wilczyńska and K. Siwek-Wilczyńska, Phys. Lett. 55B, 270 (1975).

[12]W. D. Myers, Nucl. Phys. A204, 465 (1973).

[13]P. Sperr, T. H. Braid, Y. Eisen, D. G. Kovar, F. W. Prosser, Jr., J. P. Schiffer, S. L. Tabor, and S. Vigdor, Phys. Rev. Lett. 37, 321 (1976).

Spectra of Very Highly Charged Cu- and Zn-Like Ions

Joseph Reader and Gabriel Luther

National Bureau of Standards, Washington, D. C. 20234

(Received 5 June 1980)

The $4s$-$4p$, $4p$-$4d$, and $4d$-$4f$ transitions of ten copperlike and zinclike ions from Ba^{26+} to W^{45+} have been observed by means of a laser-produced plasma and a 2.2-m grazing-incidence spectrograph. The spectra are accompanied by a prominent continuum lying just below the $4p\,^2P_{1/2}$-$4d\,^2D_{3/2}$ transitions in the copperlike ions. The results support the identification of the resonance lines of Xe^{24+} and Xe^{25+} in the Princeton University ST tokamak by Hinnov.

PACS numbers: 32.30.-r, 52.70.-m, 52.50.Jm

The spectra of ions having simple atomic structures are currently of great interest because of their use in the diagnosis of hot plasmas found in controlled-fusion devices. Of special importance are ions in the copper and zinc isoelectronic sequences. These ions contain one and two elec-

trons, respectively, outside tightly bound closed shells and their spectra thus remain simple, even for very highly ionized species.

Until recently very little experimental data were available for Cu- and Zn-like ions, especially for highly stripped species. With the exception of the observation of the $4s$-$4p$ resonance transitions of Mo^{12+}, Mo^{13+}, Xe^{24+}, and Xe^{25+} in the Princeton University ST tokamak[1,2] the $4s$-$4p$ resonance transitions in the Cu sequence were known[3,4] only through Rb^{8+}. In the Zn sequence they were known only through Kr^{6+}. In 1977, Reader and Acquista[5] used a vacuum spark and a 10.7-m grazing-incidence spectrograph to extend observation of the $4s$-$4p$ transitions to Mo^{12+} and Mo^{13+}, which confirmed the Mo identifications in Refs. 1 and 2. More complete analyses for Kr^{7+}, Y^{10+}, Zr^{11+}, Nb^{12+}, and Mo^{13+} (Refs. 6–10) have since been reported.

In this Letter we report observation of the $4s$-$4p$ resonance lines and other $n=4\rightarrow 4$ transitions in ten Cu-like and Zn-like ions from Ba^{26+} to W^{45+}. The W^{45+} ion is now the highest charge state to be studied by optical spectroscopic techniques; that is, with diffraction gratings. The results provide experimental data for the evaluation of recent relativistic calculations. They should also be of interest for tokamaks in which tungsten is used as a limiter material.

The ions in the present experiment were generated by focusing the 1.06-μm light from a large Nd:glass laser at the Los Alamos Scientific Laboratory onto flat metallic targets. Typical laser pulses had an energy of 30 J and a duration of 300 ps. The laser beam was focused onto the targets by a single aspheric lens of 200 mm focal length.

The spectra were recorded on Kodak 101-05 photographic plates with a 2.2-m grazing-incidence spectrograph. The angle of incidence was 87.5°. The grating had 1200 lines/mm, providing a plate factor of 0.54 Å/mm at 80 Å. Six laser shots were used for each spectrum. Wavelength calibration in the region from 10 to 120 Å was obtained from spectra of the ions Fe^{14+}–Fe^{23+}. Above 120 Å spectra of Mo^{6+} and Mo^{7+} from a low-voltage sliding spark were used for calibration. The internal consistency of the measured calibration lines was 0.005 Å. However, to account for possible shifts between the calibration and unknown spectra the uncertainty of the measured wavelengths is estimated as ± 0.02 Å.

Figure 1 shows a densitometer trace of the $n=4\rightarrow 4$ spectra observed in Nd, Gd, Er, and W. The signal-to-noise ratio is low in W, but the lines are clearly distinguishable on the original plates. For most of the atoms the ionization stages were confirmed by the presence of $n=4\rightarrow 5$ transitions in the Cu-like species at shorter wavelengths (20–40 Å) and by the presence of the $3d^{10}$-$3d^{9}4p$ resonance lines of Ni-like species at still shorter wavelengths (10–20 Å). In Ta and W no lines were observed outside the $n=4\rightarrow 4$ region, except for impurity lines of C^{4+} and C^{5+}.

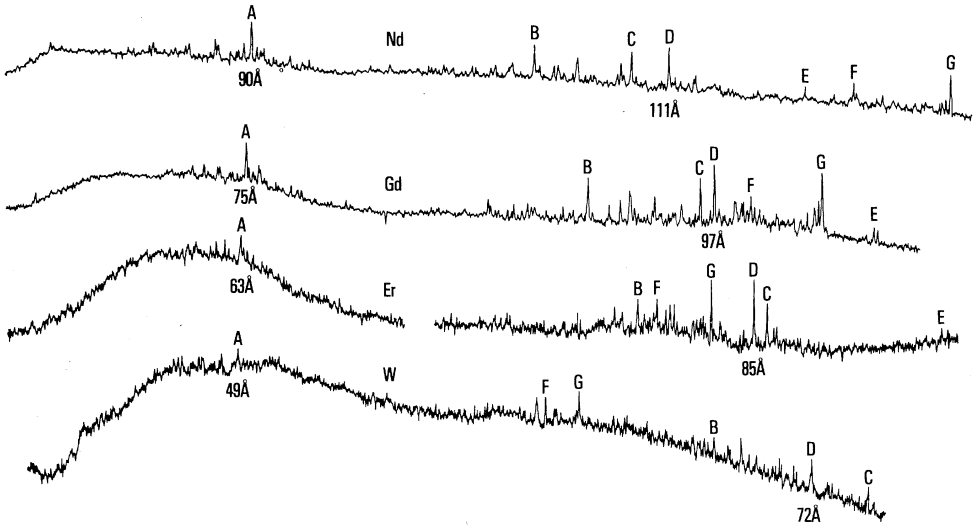

FIG. 1. $n=4\rightarrow 4$ transitions in Cu- and Zn-like Nd, Gd, Er, and W: *A*, $4p\,^2P_{1/2}$–$4d\,^2D_{3/2}$; *B*, $4d\,^2D_{3/2}$–$4f\,^2F_{5/2}$; *C*, $4d\,^2D_{5/2}$–$4f\,^2F_{7/2}$; *D*, $4p\,^2P_{3/2}$–$4d\,^2D_{5/2}$; *E*, $4p\,^2P_{3/2}$–$4d\,^2D_{3/2}$ (tentative identifications); *F*, $4s^2\,^1S_0$–$4s4p\,^1P_1$; *G*, $4s\,^2S_{1/2}$–$4p\,^2P_{3/2}$.

TABLE I. Wavelengths for the $4s^2\,{}^1S_0$–$4s4p\,{}^1P_1$ transitions of highly ionized Zn-like ions. The calculated values are from Shorer and Dalgarno, Refs. 14 and 15.

Ion	λ_{expt} (Å)	λ_{calc} (Å)
Ba^{26+}	147.94	147.28
La^{27+}	140.47	
Nd^{30+}	120.58	120.03
Sm^{32+}	109.11	108.59
Gd^{34+}	98.87	
Dy^{36+}	89.65	89.13
Er^{38+}	81.33	
Yb^{40+}	73.85	
Ta^{43+}	63.95	63.50
W^{44+}	60.98	60.52

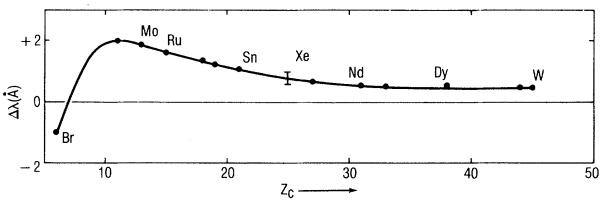

FIG. 2. Differences between observed and calculated wavelengths of the $4s^2\,{}^1S_0$–$4s4p\,{}^1P_1$ resonance line in Zn-like ions. Calculated wavelengths are from Refs. 14 and 15. The interpolated difference for Xe is indicated with an error bar.

For the higher-Z atoms studied a prominent continuum was observed just below the $4p\,{}^2P_{1/2}$–$4d\,{}^2D_{3/2}$ transitions in the Cu-like ions (see Fig. 1). In Er and W a weaker component of this continuum at longer wavelengths is seen. Similar continua have been observed in tokamaks having W limiters.[11,12] These continua have recently been attributed[13] to blending of the many lines of the $4d^{10}4f$-$4d^9 4f^2$ transition array of W XXVII.

The wavelengths of the $4s^2\,{}^1S_0$–$4s4p\,{}^1P_1$ transitions of the observed Zn-like ions are given in Table I. The experimental values are compared here with the values calculated by Shorer and Dalgarno[14,15] by means of the relativistic random-phase approximation. In Fig. 2 the differences between the observed and calculated values are plotted for the ions from Br^{6+} to W^{44+}. Z_c is the net charge of the ionic core; $Z_c = Z - N_e + 1$, where N_e is the total number of electrons in a particular ion. The points for Ru^{14+} to Sn^{20+} are from unpublished observations of the present authors. The interpolated correction to the theory for Xe is indicated with an error bar whose magnitude represents an estimate of the largest possible fluctuation of the curve between the adjacent experimental points.

The wavelengths of the $n = 4 \rightarrow 4$ transitions in four of the ten observed Cu-like ions are given in Table II. In the last column of Table II we give the values calculated by Cheng and Kim[16] for W^{45+} with the Dirac-Hartree-Fock method. Except for $4s\,{}^2S_{1/2}$–$4p\,{}^2P_{3/2}$, the agreement is excellent. The differences between the observed and calculated values for $4s\,{}^2S_{1/2}$–$4p\,{}^2P_{3/2}$ are plotted from Kr^{7+} to W^{45+} in Fig. 3.

The variation of the $4s$-$4p$ transitions through the entire Cu and Zn isoelectronic sequences is shown in Fig. 4. The $4s\,{}^2S_{1/2}$–$4p\,{}^2P_{1/2}$ transitions have actually not been observed past Ag^{18+}, except for Xe^{25+} (Ref. 2). The points for this transition past Ag^{18+} are values derived from the $4p\,{}^2P_{1/2}$ energy level as evaluated from other transitions in each ion (for example, $4p\,{}^2P_{1/2}$–$5s\,{}^2S_{1/2}$ and $4p\,{}^2P_{1/2}$–$4d\,{}^2D_{3/2}$). Data for these other transitions will be given elsewhere. The dashed line from Er to W represents an extrapolation based on the theoretical values of Cheng

TABLE II. Wavelengths in angstroms for highly ionized Cu-like ions. The calculated values for W^{45+} are from Cheng and Kim, Ref. 16. The values for $4p\,{}^2P_{3/2}$–$4d\,{}^2D_{3/2}$ are tentative.

Transition	Nd^{31+}	Gd^{35+}	Er^{39+}	W^{45+}	W^{45+}(calc.)
$4s\,{}^2S_{1/2}$–$4p\,{}^2P_{3/2}$	125.90	102.50	83.81	62.39	61.94
$4p\,{}^2P_{1/2}$–$4d\,{}^2D_{3/2}$	89.84	75.32	63.40	49.27	49.20
$4p\,{}^2P_{3/2}$–$4d\,{}^2D_{3/2}$	117.94	105.13	94.74		
$4p\,{}^2P_{3/2}$–$4d\,{}^2D_{5/2}$	110.78	97.07	85.76	72.05	71.94
$4d\,{}^2D_{3/2}$–$4f\,{}^2F_{5/2}$	103.79	90.93	80.46	67.93	67.94
$4d\,{}^2D_{5/2}$–$4f\,{}^2F_{7/2}$	108.82	96.40	86.38	74.52	74.50

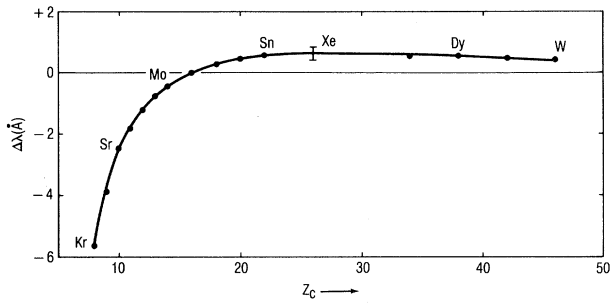

FIG. 3. Differences between observed and calculated wavelengths of the $4s\,^2S_{1/2}$–$4p\,^2P_{3/2}$ resonance lines of Cu-like ions. Calculated values are from Ref. 16. The interpolated difference for Xe is indicated with an error bar.

and Kim.[16] As pointed out in Ref. 5, the energy shifts for $4s\,^2S_{1/2}$ and $4p\,^2P_{1/2}$ due to relativity largely cancel out in the transition energy, resulting in a nearly linear variation of the transition energy with Z_c. The relatively long wavelength of this transition results in a low theoretical intensity, which probably accounts for our failure to observe it in the heavier ions.

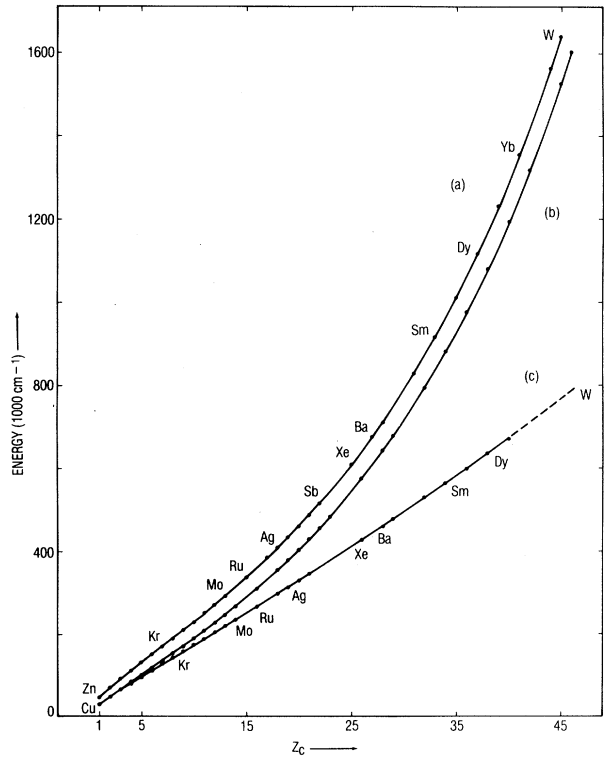

FIG. 4. Z dependence of the energies of resonance transitions in the Cu and Zn isoelectronic sequences. Curve a, $4s^2\,{}^1S_0$–$4s4p\,{}^1P_1$ of the Zn sequence. Curve b, $4s\,{}^2S_{1/2}$–$4p\,{}^2P_{3/2}$ of the Cu sequence. Curve c, $4s\,{}^2S_{1/2}$–$4p\,{}^2P_{1/2}$ of the Cu sequence.

TABLE III. Predicted and observed wavelengths of the $4s$–$4p$ resonance lines of Xe^{24+} and Xe^{25+}.

Ion	Transition	λ_{pred} (Å)	λ_{obs} (Å)[a]
Xe^{24+}	$4s^2\,{}^1S_0$–$4s4p\,{}^1P_1$	164.4 ± 0.2[b]	164.5 ± 0.5
Xe^{25+}	$4s\,{}^2S_{1/2}$–$4p\,{}^2P_{3/2}$	173.9 ± 0.2[c]	173.9 ± 0.5
Xe^{25+}	$4s\,{}^2S_{1/2}$–$4p\,{}^2P_{1/2}$	233.9 ± 0.2[d]	234.2 ± 0.5

[a] E. Hinnov, Ref. 2.

[b] Value (163.62 Å) of Shorer and Dalgarno, Ref. 14, plus a correction of 0.8 ± 0.2 Å.

[c] Value (173.3 Å) of Cheng and Kim, Ref. 16, plus a correction of 0.6 ± 0.2 Å.

[d] Value (232.4 Å) of Cheng and Kim, Ref. 16, plus a correction of 1.5 ± 0.2 Å.

In Table III, we compare the values for the $4s$–$4p$ transitions of Xe^{24+} and Xe^{25+} predicted by adjusting the theoretical values according to the interpolated corrections in Figs. 2 and 3 with the tokamak observations of Hinnov.[2] The correction for $4s\,^2S_{1/2}$–$4p\,^2P_{1/2}$ of Xe^{25+} was taken from a curve similar to that in Fig. 3. The predicted values in Table III support Hinnov's identifications very well.

We would like to thank Dr. J. McNally and Dr. R. Goodwin for making the Los Alamos laser available. We are grateful to Dr. Albert Engelhardt for his generous cooperation in operating the laser and arranging the technical aspects of our work at Los Alamos. The efforts of R. Robertson and I. V. Johnson in operating the laser are also greatly appreciated. This work was supported in part by the U. S. Department of Energy.

[1] E. Hinnov, L. C. Johnson, E. B. Meservey, and D. L. Dimock, Plasma Phys. 14, 755 (1972).

[2] E. Hinnov, Phys. Rev. A 14, 1533 (1976).

[3] C. E. Moore, *Atomic Energy Levels*, U. S. National Bureau of Standards Circ. No. 467 (U. S. GPO, Washington, D. C., 1958), Vol. II.

[4] B. C. Fawcett, B. B. Jones, and R. Wilson, Proc. Phys. Soc. London 78, 1223 (1961).

[5] J. Reader and N. Acquista, Phys. Rev. Lett. 39, 184 (1977).

[6] A. E. Livingston, L. J. Curtis, R. M. Schectman, and H. G. Berry, Phys. Rev. A 21, 771 (1980).

[7] J. Reader and N. Acquista, J. Opt. Soc. Am. 69, 1285 (1979).

[8]J. Reader and N. Acquista, J. Opt. Soc. Am. 69, 1659 (1979).
[9]J. Reader and N. Acquista, J. Opt. Soc. Am. 70, 317 (1980).
[10]J. Reader, G. Luther, and N. Acquista, J. Opt. Soc. Am. 69, 144 (1979).
[11]R. C. Isler, R. V. Neidigh, and R. Cowan, Phys. Lett. 63A, 295 (1977).
[12]E. Hinnov and M. Mattioli, Phys. Lett. 66A, 109 (1978).
[13]J. Sugar and V. Kaufman, Phys. Rev. A 21, 2096 (1980).
[14]P. Shorer and A. Dalgarno, Phys. Rev. A 16, 1502 (1977).
[15]P. Shorer, Phys. Rev. A 18, 1060 (1978). This paper contains excitation energies for Zn-like Ga, Br, Mo, W, and U. Values for intermediate atoms were communicated privately by the author.
[16]K. T. Cheng and Y.-K. Kim, At. Data Nucl. Data Tables 22, 547 (1978).

Transmission of Fast H_2^+ through Thin Foils

N. Cue,[a] N. V. de Castro-Faria,[b] M. J. Gaillard, J.-C. Poizat, and J. Remillieux
Institut de Physique Nucléaire (et Institut National de Physique Nucléaire et de Physique des Particules), Université Lyon-I, F69622 Villeurbanne, France

and

D. S. Gemmell and I. Plesser[c]
Physics Division, Argonne National Laboratory, Argonne, Illinois 60439
(Received 14 March 1980)

Transmission yield of fast H_2^+ through carbon foils has been measured over a wide range of foil thicknesses for 0.4–1.2-MeV/amu H_2^+ projectiles. A model is described which gives an excellent quantitative account of this yield as well as that of the associated H^0 production.

PACS numbers: 34.50.Hc, 34.70.+e, 79.20.Rf

Evidence recently accumulated[1-3] has demonstrated that simple atoms and molecules transmitted through thin solids at velocities $V > v_0$, where v_0 is the Bohr velocity, can be the incident species with their original electron(s) as well as those reconstituted by the process of target electron capture after the loss of the incident electron(s). For convenience, we distinguish the two as the $\mathcal{O}$ (original) and $\mathcal{R}$ (reconstituted) transmission regimes, respectively. The $\mathcal{O}$ regime may be simply characterized by the survival of the incident projectile and this has been described in detail elsewhere.[1-3] The $\mathcal{R}$ regime may not be so simply understood except perhaps for the case of atomic projectiles. Indeed, data on molecular transmission in the $\mathcal{R}$ regime have been available[4-8] for a number of years and, to our knowledge, no quantitative account has previously been given for the yield of even the simplest case of H_2^+. We describe here a quantitative model for fast H_2^+ which reproduces remarkably well the observed transmitted yield of H_2^+ as well as the associated yield of H^0 breakup fragments.

The experimental features of the H_2^+ transmitted fraction at 0.4, 0.8, and 1.2 MeV/amu through carbon foils 1–8 $\mu g/cm^2$ thick are shown in Fig. 1 as a function of dwell time, t_D, in the target. These new data were obtained at Université Lyon-I using a procedure described elsewhere.[3] The $\mathcal{O}$ and $\mathcal{R}$ features can clearly be seen. There is the $\mathcal{O}$ region of $t_D \lesssim 1$ fs which is observed to follow $\exp(-t_D/\tau)$, with $\tau = 0.17$ fs, independently of the projectile velocity V. This translates into an "electron-loss" cross section $\sigma_l \propto 1/V$ which is a feature expected from binary collisions.[1] On the other hand, there is the other region of $t_D > 1$ fs, which exhibits a strong dependence on V. Such a feature can only be reasonably understood in terms of a reconstitution process after the loss of the incident electron, and it is this process that is of principal concern here.

To properly focus on the $\mathcal{R}$ regime, we subtract out the exponential $\mathcal{O}$ transmission yield from the data and display in Fig. 2(b) the $\mathcal{R}$ transmission yield $Y(H_2^+)$ relative to twice the equilibrium neutral fraction Φ_0 for incident H^+ of the corresponding velocity. In effect then we have made use of a previous observation[6] that the

